Physics Letters A 380 (2016) 322–325

Contents lists available at ScienceDirect

Physics Letters A

www.elsevier.com/locate/pla

Observation of beam deflection in one-dimensional photonic lattice in $LiNbO_3$ crystal accompanied with self-focusing and self-defocusing nonlinearities

Yongqi Liu [a], Xinyuan Qi [a,*], Yang Lu [a], Zheng Cao [b,c], Shasha Li [a], Jintao Bai [a,b]

[a] School of Physics, Northwest University, Xi'an, Shaanxi 710069, China
[b] Institute of Photonics & Photon-Technology, Northwest University, Xi'an, Shaanxi 710069, China
[c] National Key Laboratory of Science and Technology on Space Microwave, CAST, Xi'an, Shaanxi 710100, China

ARTICLE INFO

Article history:
Received 16 May 2015
Received in revised form 21 September 2015
Accepted 7 October 2015
Available online 20 October 2015
Communicated by V.A. Markel

Keywords:
Photonic lattice
Self-focusing
Self-defocusing
Deflection

ABSTRACT

We numerically and experimentally investigated the deflection of a laser beam in a photo-induced one dimensional (1D) photonic lattice (PL) in a pure $LiNbO_3$ crystal accompanied with self-focusing and self-defocusing nonlinearities, respectively. The results show that the probe beam will be self-focused or self-defocused when the sample temperature is increased or decreased. Moreover, the light beam deflects to the direction of heat flux if there exists an additional temperature difference between the two lateral sides of the sample. The probe beam forms a deflected discrete circle soliton in the PL when the sample temperature is increased from 25 °C to 45°C and the additional temperature difference is ±5 °C. Our simulation results are in agreement with the experimental observation.

1. Introduction

Light propagation in periodic optical medium, such as fabricated waveguide arrays and optically induced photonic lattices (PL), is very different from that in homogeneous media due to the photonic band gap effects [1,2]. Usually, some homogeneous mediums, such as strontium barium niobate (SBN), lithium niobate ($LiNbO_3$) crystals and films, were widely used to study the discrete solitons, pyroelectric soliton and fast-beam self-trapping under the photorefractive and pyroelectric nonlinearity [3–7]. Recently, lattice surface solitons in diffusive nonlinear media, as well as soliton dynamics in parity-time (PT) symmetric lattices, have been studied theoretically [8,9]. Therefore, soliton dynamics in lattices is still an attractive topic in optics.

Deflected beam is a kind of beam whose propagation behavior differs from the conventional one. It was first predicted that a light beam with an asymmetric intensity profiles incident upon a material with an intensity-dependent refractive index would consequently curve its own trajectory [10]. Consistent with this theory, this effect was first observed in a NaCl crystal [11]. Later, self-deflections of the light beam had also been demonstrated in CdS_xSe_{1-x} semiconductor crystals, nonlinear liquid CS_2, sodium vapour, nematic liquid-crystal films [12–15]. In previous years, a large deflection of a broad beam and self-bending of the soliton beams were also achieved in biased crystals [16–19]. Self-bending of photorefractive (PR) soliton and mobility of solitons undergoing non-local diffusive nonlinearity in PR medium are contributed to the diffusion [17–19]. The soliton deflection in the crystal with a low concentration of deep traps was attributed to the asymmetric internal space charge field under the biased external field [18,19]. Recently, single-beam deflection has been obtained in the nonsymmetric photonic crystal gratings made of isotropic linear materials [20]. Self-deflection of solitons, beam and plasmonic lattice solitons have also been studied and observed in periodic optical medium [21,22].

In this paper, we numerically investigated and experimentally observed the self-deflection of a laser beam in a photo-induced (1D) PL in a pure $LiNbO_3$ (LN) crystal accompanied with self-focusing and self-defocusing nonlinearities, respectively. The self-focusing and self-defocusing PR effects in $LiNbO_3$ crystal are controlled by the pyroelectric effect caused by the temperature change of the sample [6]. If there exists an additional temperature difference between the two lateral facets of the sample, the beam deflects along the ***c*** axis of the crystal due to the thermo-optic effect.

* Corresponding author. Tel.: +86 29 8830 2343.
E-mail address: qixycn@nwu.edu.cn (X. Qi).

http://dx.doi.org/10.1016/j.physleta.2015.10.025

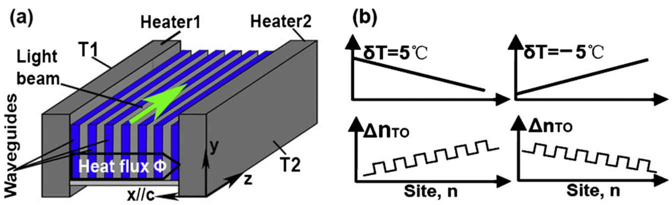

Fig. 1. (a) Schematic of a light beam in 1D photo induced PL. T_1 and T_2, the temperatures of the two lateral sides of the crystal; $\boldsymbol{\phi}$, the vector of heat flux; $\boldsymbol{c}$, the crystal axis; x and y, the axes in the transverse plan; z, the axis in the propagation direction. (b) Schematics of the temperature distributions and refractive index distribution in the crystal. δT, the temperature difference of the two lateral sides; Δn_{TO}, the refractive index distribution caused by the thermo-optic effect; Site n, the waveguide number.

2. Theoretical analysis

The PR crystals usually exhibit the photovoltaic effect, pyroelectric effect, and other nonlinear effects simultaneously [23–25]. In typical PR media, e.g., LN crystal, the value of the space-charge electric field can be obtained from the Kukhtarev–Vinetskii model [26] and it can be solved by a triple integration [6,16,19]. When illuminated with a light intensity distribution I, evolution of the charge density ρ is given by

$$\frac{\partial \rho}{\partial t} = -\mu e \nabla (N \cdot \boldsymbol{E}_{sc}) - \beta_{ph} \nabla \left[\left(N_d - N_d^+ \right) I \right] \cdot \boldsymbol{c}, \quad (1)$$

where N is the free electron density, N_d is the total donor density, N_d^+ is the ionized donor density, μ is the electron mobility, β_{ph} is the photovoltaic coefficient, e is the electron charge and $\boldsymbol{c}$ is the unit vector of the crystalline axis. If the temperature of LN crystal is changed, the total internal space charge field in LN crystal is decided by [19]

$$\boldsymbol{E}_{sc}(\boldsymbol{r}) = E_{py} \cdot \boldsymbol{c} + \frac{1}{4\pi \varepsilon \varepsilon_0} \iiint\limits_V \rho(\boldsymbol{r}) \frac{\boldsymbol{r} - \boldsymbol{r}'}{|\boldsymbol{r} - \boldsymbol{r}'|^3} dV, \quad (2)$$

where ρ is the charge density and $\boldsymbol{r}$ is the position vector. The pyroelectric charge field E_{py} is given by [23,24] $E_{py} = -\frac{1}{\varepsilon \varepsilon_0} p \Delta T$, where ε is the static dielectric constant, ε_0 is the permittivity of free space, p is the pyroelectric coefficient, ΔT is the deviation of the sample from the temperature beginning from T_0, $\Delta T = T_1 - T_0$. By increasing or decreasing the temperature of the sample, E_{py} can be positive or negative. Therefore, the self-focusing effect of the LN crystal could be enhanced or suppressed by adjusting the sample temperature.

If there exists an additional temperature difference δT between the two lateral facets of the crystal, the heat flux travels from the hot to the cold facets [Fig. 1(a)]. $\boldsymbol{\phi}$ denotes the vector of heat flux. The refractive index modulation Δn_{TO} induced by the additional temperature difference δT between the two lateral facets of the crystal could be attributed to the thermo-optic effect [28]. It is given by $\Delta n_{TO} = \frac{dn}{dT} \delta T$, where $\frac{dn}{dT} = -10^{-4}\ \mathrm{K}^{-1}$ is the temperature coefficient of the refractive index. In turn, $\delta T = T_1 - T_2$, where T_1 and T_2 denote the temperatures of the two lateral sides (see Fig. 1(a)). If there exists a temperature deviation between the two lateral sides of the crystal ($T_1 \neq T_2$), the additional temperature difference δT should be considered. The case of $T_1 > T_2$, δT is positive; Otherwise, $T_1 < T_2$, δT is negative. Fig. 1(b) shows the distribution sketch between the refractive index caused by the thermo-optic effect and the temperature difference [27]. Apparently, the algebra sign of Δn_{TO} is always opposite to that of δT as shown in Fig. 1(b).

In the photo induced 1D PL, the total refractive index modulation Δn in the whole crystal volume can be expressed as [28]

$$\Delta n = \Delta n_{sc} + \Delta n_{TO} + \Delta n_{PL} \quad (3)$$

where Δn_{sc} is the refractive index modulation induced by $\boldsymbol{E}_{sc}(\boldsymbol{r})$ through the linear Pockels effect, Δn_{PL} is the refractive index distribution of the 1D PL. Therefore, light dynamics in 1D PL in LN accompanied with the photovoltaic effect, pyroelectric effect, and the thermo-optic effect can be simplified to the propagation in the system with refractive index modulation Δn.

3. Numerical simulations

In this section we study numerically the propagation dynamics of a laser beam in 1D photo-induced PL in a pure LN crystal. The light behavior in such a system obeys the Nonlinear Schrödinger Equation. The split-step Fourier transform beam propagation method (BPM) is used by Matlab to simulate the light behavior in the nonlinear PL. The numerical model consists of focusing an extraordinarily polarized (e-polarized) Gaussian beam sat $\lambda = 532$ nm (FWMH 18 μm) located at the entrance face of a dark stripe (high refractive index region) in 1D PL pattern in a 10 mm long LN crystal. The spacing of the 1D PL is $\Lambda = 15$ μm [Fig. 2(a)]. The pyroelectric effect is taken into account when the temperature of the sample is changed. The pyroelectric coefficient p is close $-6 \times 10^{-5}\ \mathrm{C\,m^{-2}\,K^{-1}}$ [29]. Considering that the heat flux is a function of spatial coordinates, the temperature distribution along the $\boldsymbol{c}$ axis is regarded as a linear function of the position as well [27]. The refractive index perturbation at position x can be expressed by $\Delta n_{TO}(x) = \frac{dn}{dT} \delta T \frac{(x - \frac{D}{2})}{D}$, where D is the width of the axis. The amplitude of the photo induced 1D PL is described by a cosine function. The other parameters are taken from Refs. [6,18,19,30].

The simulation results are shown in Fig. 1. When the temperature of the sample is increased to 45 °C ($\Delta T = 20$ °C) and there is no additional temperature difference between the two lateral sides ($\delta T = 0$ °C), the probe beams will be self-trapped into straight elliptical shapes (1-D soliton) in 1D PL [Figs. 2(c1), (d1)]. This means the pyroelectric effect suppresses the photovoltaic effect when $\Delta T = 20$ °C. Furthermore, if $\Delta T = 20$ °C and $\delta T = -5$ °C, the probe beam will be trapped into a circular discrete soliton and travels along a bending trajectory to the direction of the heat flux [Figs. 2(c2), (d2)]. Conversely, if $\Delta T = 20$ °C and $\delta T = 5$ °C, the probe beam will be trapped into a circular discrete soliton and travels in the opposite direction [Figs. 2(c3), (d3)]. These demonstrate that the additional temperature difference δT between the two lateral sides results in the bending behavior due to the thermo-optic effect.

When $T0 = 45$ °C, $\Delta T = -20$ °C and $\delta T = 0$ °C, the facula size of the probe beam at the exit facet will be larger than that at the entrance facet [Figs. 2(c4), (d4)]. Thus, the pyroelectric effect enhances the photovoltaic effect when $\Delta T = -20$ °C. In addition, the probe beam also deflects to the direction of the heat flux if $\delta T = -5$ °C or 5 °C [Figs. 2(c5), (c6)]. These confirmed further the thermo-optic effect results into the bending of the probe beam.

4. Experiments and results

The experimental setup is sketched in Fig. 3. Two CW lasers with wavelength of 532 nm are used as the light sources. The e-polarized beam from Laser1 is split into two parts and they interfere at the input facet of the crystal. The period of the 1D interference patterns is approximately $\Lambda \approx 15$ μm. The e-polarized beam from Laser2 is also split into two parts. One is focused to 18 μm FWHM with power of about 200 μW onto a certain position of the input face of the crystal by a spherical lens L1 as the probe beam; the other is used as the read-out beam to detect the waveguide in the sample. The sample is a pure LN crystal with dimensions of 2 mm × 10 mm × 10 mm along x ($\boldsymbol{c}$-axis), y and z